Front. Phys., 2014, 9(3): 385–397
DOI 10.1007/s11467-013-0381-1

REVIEW ARTICLE

Material transport in dip-pen nanolithography

Keith A. Brown[1,2], **Daniel J. Eichelsdoerfer**[1], **Xing Liao**[2,3], **Shu He**[1], **Chad A. Mirkin**[1,2,3,†]

[1] *Department of Chemistry, Northwestern University, 2145 Sheridan Road, Evanston, IL 60208, USA*
[2] *International Institute for Nanotechnology, Northwestern University, 2145 Sheridan Road, Evanston, IL 60208, USA*
[3] *Department of Materials Science and Engineering, Northwestern University, 2145 Sheridan Road, Evanston, IL 60208, USA*
Corresponding author. E-mail: [†] *chadnano@northwestern.edu*
Received May 28, 2013; accepted August 16, 2013

Dip-pen nanolithography (DPN) is a useful method for directly printing materials on surfaces with sub-50 nm resolution. Because it involves the physical transport of materials from a scanning probe tip to a surface and the subsequent chemical interaction of that material with the surface, there are many factors to consider when attempting to understand DPN. In this review, we overview the physical and chemical processes that are known to play a role in DPN. Through a detailed review of the literature, we classify inks into three general categories based on their transport properties, and highlight the myriad ways that DPN can be used to perform chemistry at the tip of a scanning probe.

Keywords dip-pen nanolithography, scanning probe lithography, materials transport

PACS numbers 07.79.Lh, 68.35.Fx, 73.40.-c

Contents

1 Introduction

The ability to pattern surfaces with functional materials is of central importance to many areas of science and technology. Of the numerous lithographic tools that have been developed to address this need, dip-pen nanolithography (DPN) is the direct-write molecular printing technique with the highest resolution [1]. By coating a scanning probe tip with molecules of interest, these molecules can be selectively transferred to a surface through the meniscus that spontaneously condenses between the tip and substrate under ambient conditions. In analogy to writing with a hand-held pen, in DPN, a scanning probe is considered a "pen" and is coated with molecules or a solution of molecules known as the "ink." This technique allows one to pattern materials with the precise registration afforded by piezoelectric positioning and with feature sizes down to 10 nm, all in a mask-free and biocompatible fashion [2, 3]. Following this initial observation, the resulting explosion of research into DPN revealed that a broad range of materials could be patterned on a diverse set of surfaces [3, 4]. The ability to directly deposit a wide variety of materials in a mask-free fashion has made DPN useful for synthesizing biomolecular nanoarrays, templating cellular recognition sites, and constructing combinatorial arrays of both organic and

Frontiers of Physics

inorganic materials [3, 4]. Part of the reason for the widespread adoption of DPN is that it has a low barrier to entry; any researcher with access to an atomic force microscope (AFM) can perform a DPN experiment and thus print nanoscale features.

Concurrent with the increase in applications of DPN, much work has focused on developing an understanding of the interesting physical and chemical phenomena involved in the DPN process. This review is intended to summarize this progress by outlining the current understanding of DPN and serve as a starting point for researchers who would like to explore the patterning of new materials. Other literature reviews can be referred to for a more in-depth look at the evolution [3] of DPN or its applications [4, 5]. While DPN originally utilized cantilever-based scanning probes, recent breakthroughs have transitioned many molecular printing experiments onto cantilever-free platforms that offer higher throughput while maintaining the disposable nature of the probes [6–8]. While the development and application of cantilever-free lithographic techniques are beyond the scope of this review [9], the principles discussed herein apply to both cantilever-based and cantilever-free molecular printing tools.

This review proceeds as follows: Section 2 contains an overview of the basic physical models of material transport in DPN. Section 3 presents a discussion of the physical factors that influence transport in DPN and delineates three categories of inks. Section 4 outlines the diversity of chemistry that has been performed at the tip of a scanning probe and details how these chemical considerations affect patterns generated by DPN. We conclude with a brief discussion of the open questions related to materials transport in DPN.

2 Modeling the DPN process

DPN is a materials transport process, and the manner in which materials are transferred from the scanning probe tip to the substrate involves both physical and chemical interactions. The basic picture is that when an ink-coated AFM tip is brought into contact with a surface, material will transport from the tip to the surface in a controlled fashion. Depending on the ink, two physical phenomena, molecular diffusion and fluid flow, may take place. The relative importance of these effects depends considerably on the ink material in question. In the case where molecular diffusion dominates, the ink is known as a diffusive ink while in the case when fluid flow dominates, the ink is known as a liquid ink. In this section, we outline models of these two effects.

2.1 Transport models for diffusive inks

In a typical DPN experiment with a diffusive ink, an AFM probe is dipped into an ink solution for a specified amount of time. Following dip coating, the solvent evaporates, leaving a well-defined quantity of ink molecules on the tip, defined here as the ink loading. The AFM probe is then loaded into a scanning probe instrument with both temperature- and humidity-control. When the tip is brought into contact with a surface, a water meniscus spontaneously forms and ink diffuses from the tip to the surface [Fig. 1(a)] [10]. To generate a dot feature, the AFM tip is held in contact with the substrate for a specified dwell time. To generate a line, the tip is brought into contact with the surface and moved across the surface at a constant velocity known as the writing speed. These features are characterized by their diameter (for dots) or their width (for lines).

Depositing diffusive inks is hypothesized to encompass three processes [11]: (1) *Dissolution*: ink molecules dissolve from the tip into the water meniscus. This is a kinetic process in which the ink molecules are thermally activated [12]. (2) *Diffusion*: ink molecules diffuse through the water meniscus from the tip to the surface and then along the surface. This process is assumed to be Fickian and therefore the flux of material is expected to be proportional to the difference in ink concentrations between the tip and the surface. (3) *Assembly*: ink molecules in the vicinity of the surface bind to any available site through a thermally activated process.

Many analytical and numerical models of DPN of diffusive inks have been proposed that make quantitative predictions relating feature size to patterning and material parameters [13]. The results of these models can be contextualized by considering their assumptions regarding the relative rates of the steps in the three step process described above. For example, the first model of DPN, proposed by Jang *et al.*, utilized a surface diffusion model of steps (2) and (3) with the assumption that a constant flux of material was delivered to the surface [13]. We interpret this assumption to be a "dissolution-limited" case because steps (2) and (3) are assumed to be sufficiently fast that there is never a downstream buildup of material that would slow dissolution. Under these assumptions, they found that the feature diameter will grow linearly with time to the 1/2 power, but that the slope of this growth would depend on whether step (2) or step (3) was faster.

In a different model, Cho *et al.* considered the case when the tip is treated as having a constant concentration of dissolved ink [14]. We consider this to be a fast dissolution condition as step (1) must occur sufficiently

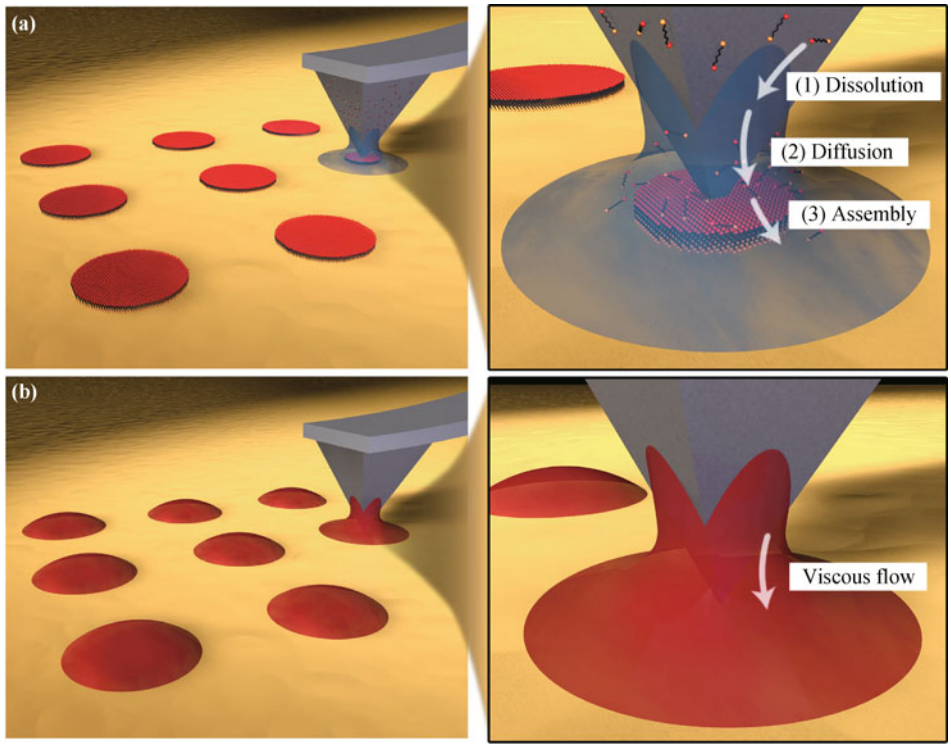

Fig. 1 **(a)** Schematic of dip-pen nanolithography (DPN). A patterning experiment in which a soluble small molecule ink is deposited consists of three steps: (1) *Dissolution* in which the ink dissolves into the water meniscus. (2) *Diffusion* during which the ink diffuses from the tip to the surface. (3) *Assembly* in which the ink absorbs to the surface. **(b)** Schematic depicting the patterning of liquid ink materials by DPN.

fast such that the ink concentration at the tip quickly saturates. Interestingly, the dynamics of feature growth in this model were dominated by the relative importance of steps (2) and (3): in the "diffusion-limited" case where step (3) was much faster than step (2), they predicted that the diameter of a feature should grow as time to the 1/2 power while in the "assembly-limited" case where step (2) was much faster than step (3), the power law exponent was expected to decrease to 1/3.

The relative importance of the steps in the DPN process are not determined solely by material parameters; patterning conditions such as dwell time can change the appropriate physical model. For example, Weeks *et al.* developed a model of the dissolution kinetics by comparing the combined rate of steps (2) and (3) to that of step (1) [12]. By modeling dissolution as a first order process, they found that the same system could be considered "dissolution-limited" or "diffusion-limited" depending on the dwell time. At early times, they observed a constant flux of material from the tip while at later times, they observed a constant concentration of ink in solution. Under both asymptotic conditions, they predicted that the feature diameter would grow linearly with time to the 1/2 power, but that the slope of this growth would slow at the transition from constant flux to constant concentration [12]. A later model by Saha *et al.* treated the general case of a similar model and found a non-power law dependence of line width on writing speed [11].

The diversity of models of DPN shows that a great deal of effort has gone into understanding the transport of diffusive inks. As such, there is a fairly clear picture of the important parameters. Here, we have provided a simplified picture of DPN that does not include contributions from molecule-molecule interactions, though many additional models treat these interactions explicitly using molecular dynamics and other techniques [15–17].

2.2 Transport models for liquid inks

In contrast to diffusive inks, the transport of liquid inks is dominated by bulk fluid flow from the tip to a surface [Fig. 1(b)]. When a pen coated with a liquid ink touches a surface, a fluid flow arises that transports the ink to the surface. This flow is assumed to be influenced by many effects including the Laplace pressure at the meniscus, the surface energy, and the liquid viscosity [18]. Despite widespread use as a transport strategy in DPN, there are few models of this behavior in the literature, although analysis of this problem using a mass transfer model based on low Reynolds number fluid dynamics has

provided useful insight [18, 19]. In a recently proposed model that analyzed the fluid flow through extension of the Stokes equations, the rate of mass transfer was predicted to decrease with dwell time and ink viscosity [19]. The lack of detailed theoretical studies in this area represents an opportunity for furthering our understanding of liquid ink transport in DPN.

3 Physical considerations of materials transport

Having laid out the theoretical framework that has been used to describe the DPN process, we will now overview the experimental studies that provide insight into the factors that affect the transport rate. We will initially focus on the widely studied 16-mercaptohexadecanoic acid (MHA) as a canonical diffusive ink.

3.1 Relative humidity

Relative humidity (RH) is perhaps the most widely studied factor with respect to DPN. For MHA alone, there have been many studies that examine the effect of RH on the rate of transport. The transport rates measured in three representative studies are displayed in Fig. 2 [12, 20, 21]. The transport rate increased with RH in these experiments, and this trend was consistent despite the disparity in inking conditions that were used. Increasing the RH is hypothesized to result in a larger water meniscus, thus expediting steps (1) and (2) for water soluble materials like MHA [20]. The existence of the meniscus has been supported by compelling evidence through direct observation of the meniscus at a RH as low as 40% in an environmental scanning electron microscope (ESEM) [22, 23]. Additionally, experiments performed by placing an AFM probe in contact with a NaCl substrate at RH values as low as 0% resulted in sample etching and pull-off forces commensurate with meniscus formation [24]. Finally, at values of RH ~84%, molecular transport along the surface of the meniscus has been reported, leading to ring-like structures [25]. These results are all consistent with the general observation that higher humidity results in a larger meniscus [20].

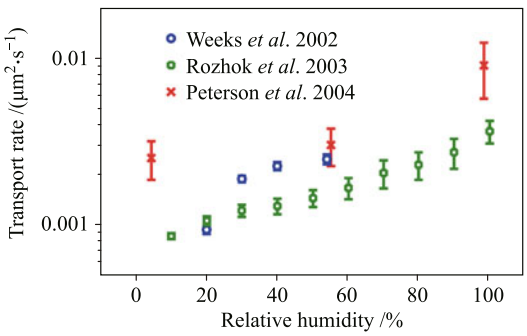

Fig. 2 Transport rate from three seminal studies in which 16-mercaptohexadecanoic acid (MHA) was patterned on gold surfaces. In each study, the rate is calculated as the slope of feature size squared vs. dwell time. The differences in rates between the three studies are presumed to result primarily from due to differences in the inking procedure used in each case.

3.2 Temperature

Given that all of the three processes in DPN are expected to depend on temperature, temperature should play a major role in determining the transport rate. Indeed, Rozhok *et al.* systematically studied the effect of temperature on MHA transfer during DPN, and as expected, the transport rate increased with increasing temperature [20]. In addition, Chung *et al.* used a heated probe and found both dissolution into the meniscus and adsorption on the surface to be thermally activated processes. In particular, they found that in the case of MHA on Au, one third of the activation barrier is from dissolution and two thirds of the barrier is from adsorption [26].

3.3 Ink loading

The ink loading is expected to be a critical factor in determining the rate of ink transfer. In the dissolution-limited case, the overall transport rate is expected to be proportional to the ink loading [11]. To study this effect, Giam *et al.* inkjet-printed various quantities of MHA onto pens and found that adding ink linearly increased the transport rate up to a saturation value [27]. As a corollary to this, it has been observed in several studies that writing for long periods of time (on the scale of hours) led to a reduction in the transport rate, presumably due to the depletion of ink reserves [21, 28, 29].

3.4 Ink composition

Thus far, the discussion has focused on the case of MHA patterned on gold. While this is an ideal model system, many additional ink-substrate combinations have been explored. In an attempt to explore the transport of a more diverse set of materials, we tabulated the rate at which a wide variety of materials were transported. A common way to parameterize the transfer rate is to print dot features with differing dwell times and find the slope of the dot diameter squared *vs.* dwell time [12]. This analysis results in a rate constant with units of length squared over time. As discussed in Section 2, this dependency is

widely seen in many models of diffusive ink transport, but is not necessarily valid for other materials. Regardless, a rate constant of this form can still be computed and used as a benchmark for transport rate.

Figure 3 shows the transport rate calculated for a selection of the materials patterned by DPN. For each material, the transport rate was either taken from the respective article, or calculated based on data presented in the article. This is not an exhaustive list of all materials that have been patterned, but rather those that have well characterized rates and were patterned under comparable experimental conditions. From lowest to highest molecular weight, the materials depicted are: 2-mercaptoimidazole [30], 4-mercaptopyridine [30], 4-amino-5-hydrazino-1,2,4-triazole-3-thiol [30], 2-mercaptobenzothiazole [30], MHA whose rate is estimated from the average rate from the studies represented in Fig. 2, cyclotetramethylene tetranitramine [25], pentaerythritol tetranitrate [31], octadecylphosphonic acid [30], coumarin 6 [32], biotin [33], rhodamine 6G [32], generation 1 (G1) poly (amido amine) (PAMAM) dendrimers [34], polyethylene glycol (PEG) whose rate is averaged from two studies [35, 36], G2 PAMAM dendrimers [34], poly(ethylene oxide)-*b*-poly(2-vinylpyridine) (PEO-*b*-P2VP) [37], G3 PAMAM dendrimers [34], G5 diaminobutane (DAB) dendrimers [34], self-doped sulfonated polyaniline (SPAN) [38], G4 PAMAM dendrimers [34], -OH terminated G4 PAMAM dendrimers [34], and two high molecular weight polymeric inks, doped polypyrrole (PPy) [38] and poly(3,4-ethylenedioxythiophene):polystyrene sulfonate [39], whose molecular weights are proprietary. It is interesting to note that, despite the disparate materials and inking conditions, general trends are apparent in the data. To analyze this data, we divide the materials studied into three categories to encompass the different behaviors observed: (1) diffusive inks, (2) aqueous liquid inks, and (3) non-aqueous liquid inks.

3.5 Diffusive inks

Diffusive inks are those whose transport is dominated by diffusion from the tip to the surface (blue crosses in Fig. 3). To classify an ink as diffusive, we required that it be soluble in water and not form domed features. For a discussion of why certain inks form flat features, the reader is referred to Section 4. Based on this classification, we observe that materials with molecular weights under ~1000 Da tend to transport with speeds in the range 0.001 to 0.1 $\mu m^2/s$, which is much slower than the bulk diffusion constant of these materials. For example, the bulk diffusion constant of MHA is 620 $\mu m^2/s$ [40], which implies that other aspects of the process must be rate-limiting. These inks form flat structures whose areas generally grow linearly with dwell time, consistent with the theoretical picture. A characteristic of diffusive inks is that since transport is presumed to be mediated by the water meniscus, the transport rate is sensitive to RH. These materials do not have to be in a liquid state to transfer, and in fact several high melting point small molecules were found to transfer readily at room temperature [30]. Significantly, this study concluded that the transport rate is primarily influenced by the material's solubility in water, further emphasizing the hypothesis and providing evidence that small molecule inks are transported through the water meniscus.

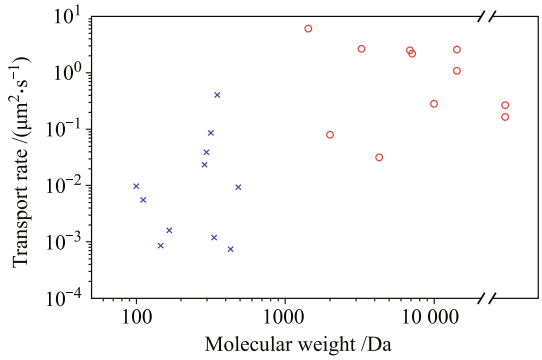

Fig. 3 Transport rates compiled for 22 different materials from 13 different studies in which each dot corresponds to a different material. For each material, the rate is calculated as the slope of feature size squared *vs* dwell time. These materials are broadly categorized as diffusive inks (blue crosses, weight <1000 Da), and aqueous liquid inks (red circles, weight >1000 Da). From lowest to highest molecular weight, the materials depicted are: 2-mercaptoimidazole [30], 4-mercaptopyridine [30], 4-amino-5-hydrazino-1, 2, 4-triazole-3-thiol [30], 2-mercaptobenzothiazole [30], MHA whose rate is estimated from the average rate from the studies represented in Fig. 2, cyclotetramethylene tetranitramine [25], pentaerythritol tetranitrate [31], octadecylphosphonic acid [30], coumarin 6 [32], biotin [33], rhodamine 6G [32], generation 1 (G1) poly (amido amine) (PAMAM) dendrimers [34], polyethylene glycol (PEG) whose rate is averaged from two studies [35, 36], G2 PAMAM dendrimers [34], poly (ethylene oxide)-*b*-poly (2-vinylpyridine) (PEO-*b*-P2VP) [37], G3 PAMAM dendrimers [34], G5 diaminobutane (DAB) dendrimers [34], self-doped sulfonated polyaniline (SPAN) [38], G4 PAMAM dendrimers [34], -OH terminated G4 PAMAM dendrimers [34], and two high molecular weight polymeric inks, doped polypyrrole (PPy) [38] and poly (3,4-ethylenedioxythiophene): polystyrene sulfonate [39], whose molecular weights are proprietary.

3.6 Aqueous liquid inks

Aqueous liquid inks are classified as those that form dome-shaped features and transfer in a humidity-dependent fashion (red circles in Fig. 3). We find that water soluble materials with molecular weights over ~1000 Da fit this category. In fact, many of these inks can-

not be transferred below a threshold value of RH [41]. This behavior is understood as arising from the material being effectively a solid when dry, with increased water content at high RH causing the material to adopt a liquid state. These materials were observed to transfer quickly compared to diffuse inks, with typical rates in the range 0.1 to 10 $\mu m^2/s$. This class of inks includes hydrophilic polymers such as PEG, amphipathic block copolymers such as PEO-*b*-P2VP, and dendrimers. These inks have the interesting property that they can be used as a transport vehicle for other materials. Examples of this include the use of PEG to transport nanoparticles [42] or fluorophores [43], the use of agarose to deposit oligonucleotides or proteins [41], and scanning probe block copolymer lithography (SPBCL) in which PEO-*b*-P2VP coordinated to a metal salt is patterned and then used as a reaction vessel for synthesizing single nanoparticles on surfaces [19, 37, 44, 45].

3.7 Non-aqueous liquid inks

Inks in which a non-volatile liquid is used as the carrier medium instead of water are classified as non-aqueous liquid inks. One might expect that the defining characteristic of this class of inks would be their viscosities. In contrast to aqueous liquid inks whose viscosity may vary due to changing water concentration from solvent evaporation, non-aqueous liquid inks are themselves composed of non-volatile solvents and therefore offer the possibility of having well-defined viscosities throughout the patterning experiment. Unfortunately, few inks in this category have been studied, but for those that have, a very interesting and counter-intuitive trend is observed (Fig. 4).

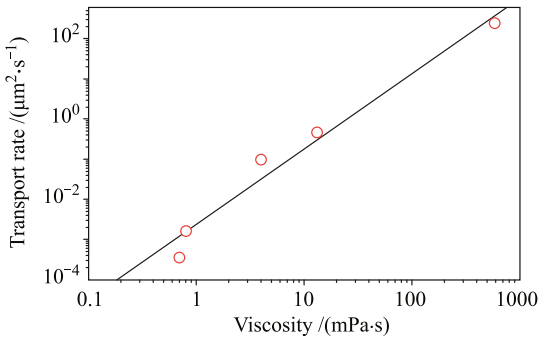

Fig. 4 Transport rates compiled for five different liquid ink materials from seven different studies in which each dot corresponds to a different material. For each material, the rate is calculated as the slope of feature size squared *vs.* dwell time. The line is a power law fit to the data with a slope of 1.8 ± 0.5. Materials are (from lowest to highest viscosity): hexamethyldisilazane (HMDS) [46], DNA in dimethylformamide (DMF) [47], the average transport rate of ODT from four studies [25, 28, 32, 46], Ag nanoparticles in glycerol [48], and polydimethylsiloxane (PDMS) diluted with hexane [49].

Non-aqueous liquid inks with higher viscosities are observed to transport faster, which is contrary to the expectation that increased viscosity would slow transport. Transport rates for five materials are represented in Fig. 4: hexamethyldisilazane (HMDS) [46], DNA in dimethylformamide (DMF) [47], the average transport rate of ODT from four studies [25, 28, 32, 46], Ag nanoparticles in glycerol [48], and polydimethylsiloxane (PDMS) diluted with hexane [49]. The viscosities of HMDS [50], DMF [51], mixtures of water and glycerol [52], and mixtures of PDMS and hexane [53] were estimated based on tabulated values.

Insoluble inks that are solids at room temperature like ODT are interesting special cases. Being insoluble in water, ODT is a poor candidate as a diffusive ink. However, the transport rate of ODT varies smoothly as the temperature is raised through its melting point, which indicates that there is no abrupt change in the transport of ODT as it melts [20]. This observation indicates that inks remain which do not fall into simple classification and thus warrant further study. To include ODT on Figure 4, its viscosity was estimated as that of an 18-unit saturated hydrocarbon [54].

The trend line in Fig. 4 has a slope of 1.8 ± 0.5, indicating that transport rate scales with viscosity to the power of ∼1.8. To explain this surprising result, we hypothesize that this is the result of the common dip-coating process used to ink tips resulting in varying film thicknesses on the tips. Indeed, in dip-coating experiments, film thicknesses are generally found to scale as the square root of the viscosity of the liquid [55]. Since the flow rate in a pressure-driven system is strongly dependent on the cross sectional area of the fluid, it is reasonable to think that this increase in thickness could result in faster flows for more viscous materials. This result stands in contrast to recent experimental work focused on a block copolymer aqueous liquid ink which revealed that the mass transport rate decreased as the viscosity of the ink increased [19]. Interpretation of these results in the framework of non-aqueous liquid inks may be difficult; however, as there is no guarantee that the viscosity of an aqueous liquid ink is constant during both inking and deposition where the concentration of water is changing during the experiment. Indeed, one may expect that inking with an aqueous liquid ink will occur in a dilute limit where the ink viscosity is relatively low whereas once the polymeric ink is dried on the tip, the viscosity is greatly increased due to the much higher effective ink concentration. To account for this, previous studies estimated the viscosity of inks with 40× higher ink concentrations than used for inking to recapitulate the highly concentrated environment of the tip-sample system [19].

Although RH is a critical parameter in the transport of diffuse inks and aqueous liquid inks, the transport rates of non-aqueous liquid inks are expected to be relatively invariant of humidity. For hydrophobic inks such as ODT and poly (vinylidenefluoride-co-trifluoroethylene) P(VDF-TrFE), the observed transport rates remain constant or slightly decrease with increasing humidity [20, 56–58]. In these and other liquid inks, the capillary bridge is expected to be composed of the material itself, rather than water. In fact, in the case of patterning 3-mercaptopropyltrimethoxysilane (MPTMS) on glass, transfer was not possible at RH >30%, which was attributed to cross linking of the MPTMS [59]. Like aqueous liquid inks, non-aqueous liquid inks have also been used as a matrix to pattern other materials. For example, glycerol has been used as an additive to pattern proteins [60, 61] and even bacteria [62].

3.8 Thermal DPN

A noteworthy approach to broadening the materials toolbox of DPN is thermal DPN, or the use of a heated tip to deposit materials that could not otherwise be deposited. In addition to providing an avenue to study the effect of temperature on transport [26], this technique has been used to pattern inks such as polymers [63–65], nanoparticle-polymer composites [66], metals [67], and solid organics [68]. Categorically, it may be appropriate to consider materials deposited in this way to be non-aqueous liquid inks that can only be transferred at temperatures above their melting or glass transition temperatures.

3.9 Other physical considerations

The three ink categories presented here are a simplified view of the factors that govern material transport in DPN. Many other factors are known to affect the transport rate. For example, surfactants in the ink such as Tween-20 have been used to aid the transport of biotin [33] and peptides [69] onto hydrophobic glass surfaces. Additionally, organic additives such as tricine have been found to accelerate transfer of agarose and allow transport at lower humidity [41]. The presence of organic vapor has also been shown to expedite transport [70]. The state of the ink material itself is also known to play a role, as dimers of R6G were found to have markedly different patterning characteristics than monomers of R6G [71]. Finally, the chemical conditions of the tip [29] and surface [72] have been shown to be important factors in determining the transport rate.

4 Chemistry at the tip of an AFM

While this review has so far focused on the physical aspects of DPN, the chemical interactions that take place between the substrate surface and the molecules on the tip of the AFM or in the meniscus play a central role in determining the patterning result. It is instructive to think of the AFM probe in DPN experiments as directing chemical reactions, and this section reviews the contributions to the field of DPN from this perspective. Not only can DPN be used to direct such reactions, but the nature of the bonding between the ink and substrate can ultimately determine the geometry of the final feature. For example, inks that undergo chemisorption typically result in flat, two-dimensional features [Fig. 1(a)] while inks that interact with the surface via physisorption result in domed, three-dimensional features [Fig. 1(b)]; indeed, it was this geometric difference that partly determined the classification of inks into three categories in the preceding sections. This difference in feature morphology is due to the relative strength of intermolecular interactions as compared to the molecular interaction with the surface. In physisorption, the van der Waals interactions between the molecules and the surface are similar in strength to the intermolecular interactions whereas, for inks that interact through chemisorption, the covalent attachment is much stronger than intermolecular forces.

When considering the broad classes of reactions one could perform with DPN, the simplest place to start is with two component reactions where a covalent bond forms between two reactant molecules. Conceptually, these are the easiest to adapt to the DPN process, as one could use one reactant in the ink, and the substrate as the other reactant. Indeed, most early DPN studies focused on this approach by patterning molecules that easily form self-assembled monolayers (SAMs) [73–76].

4.1 Self-assembled monolayers

A SAM is an ordered arrangement of a single layer of surfactant molecules on a surface. Typically, the surfactant is a small organic molecule with two functional groups separated by a long alkyl chain: the group that interacts with the surface is the “head group,” and the group at the other end is the “tail group.” The head group is often chosen based upon its ability to form a covalent bond with atoms on the surface of the substrate; this provides a thermodynamic driving force for transport and subsequent adsorption of the ink molecules on a substrate surface. The carbon chains in between the

head and tail groups pack together via van der Waals interactions, ordering the molecules into a two-dimensional crystal. The tail groups can be chosen to help dissolve the SAM molecule into a desired solvent, or they can be chosen to enable the growth of further structures by subsequent chemistry. In the context of DPN, printing SAM-forming molecules generally results in features that are topographically flat with the bond formation between the head group and the surface preventing the formation of multilayered, three-dimensional features. As a result, SAM-forming inks are generally classified as diffusive inks.

4.2 Alkanethiols on gold

The first DPN experiments involved patterning alkanethiols onto Au [1], and the two inks used in this work, ODT and MHA, became the most widely studied inks in DPN. The most appealing aspect of patterning with MHA is the fact that its terminal carboxylic acid group can be modified with further chemical reactions, and thus MHA can be used to build more complex structures. There are myriad chemical reactions that one could use to modify the COOH terminus of MHA, such as reduction, amidation, and complexation with metal ions, and one of the earliest uses of MHA in this manner was to template arrays of proteins [77]. Most of the applications of MHA patterns have focused on biological studies, and include templating single viruses [78] and studying stem cell differentiation [79].

While MHA and ODT are the most commonly used alkanethiols in DPN, it is possible to perform DPN using an alkanethiol with almost any tail group that will readily form a SAM. Some of the tail groups for alkanethiols used in DPN include amines [80, 81], thiols [82], fluorines [83], *N*-hydroxysuccinimide (NHS) ester groups [84], various aromatic rings [30], and even ferrocenyl groups [85]. These results demonstrate that, for the case of alkanethiols on Au, virtually any functional group can be patterned, and choice of the optimal tail group will depend on a variety of factors, such as solubility, melting temperature [30] and the desired coupling chemistry.

4.3 Patterning on oxides

Several early studies focused on methods for patterning oxide substrates, which are desirable both for semiconductor applications and for biological studies. The first demonstration of patterning on an oxide involved printing HMDS onto the native oxide of Si (here, SiO_x) and GaAs [46], where researchers found that HMDS was readily patterned onto semiconductor oxides, albeit at a slower rate than that for ODT onto Au. While HMDS is more air-stable than the alkylchlorosilanes and alkoxysilanes, which are the molecules that are most commonly used for functionalizing oxides [73, 74, 76], several air-sensitive silanes have also been successfully patterned including MPTMS [59, 82], 3-aminopropyldimethoxysilane (APTMS) [82], 11-(triethoxysilyl)undecanal [86], and 10-undecenyltrichlorosilane (UTCS) [87]. The authors of this last study coated their AFM probe with UTCS prior to inking, and they indicate that making the probe hydrophobic was the key to enabling transport and subsequent binding of UTCS to the surface, as a hydrophobic probe would suppress meniscus formation.

Although silanes are the most frequently utilized molecules for DPN patterning on semiconducting substrates, alkanethiols have also been patterned on III-V semiconductors. This research began by patterning cysteine-terminated peptides on GaAs [88], and continued with patterns of ODT on InP [89], GaP [90] and InAs [91]. These all required removal of the oxide immediately prior to patterning in order to take advantage of the affinity of thiol groups for clean III-V semiconductor surfaces [73, 76].

4.4 Other reactions by DPN

The formation of covalent SAMs is only a small subset of the chemical reactions that can be performed in the context of DPN. The first exploration beyond SAM formation was the demonstration of Michael addition between an acrylamide-terminated oligonucleotide and an MPTMS-coated Si wafer [47]. Many other reactions have been explored, including the Diels-Alder reaction [92], as well as amide coupling via an NHS ester [82, 93] and a carboxylic anhydride [94]. Several groups have also explored reduction/oxidation chemistry, such as using borohydride as a reductant [95], using ceric ammonium nitrate as an oxidant [96], and even using a Si wafer itself as the reductant [97].

Two-component reactions are not the only type of reaction that can be directed by DPN, however. Three-component reactions, such as reactions that require a catalyst, can also be performed with DPN. Of particular interest is the Click reaction, a term which typically refers to the Cu(I)-catalyzed Huisgen cycloaddition of an azide with an alkyne [98]. This reaction has been adopted by DPN researchers in two ways: by mixing the azide and the Cu catalyst to form an ink and writing this ink onto an alkyne-functionalized Si surface [99], and by mixing the alkyne and the Cu catalyst to form an ink and writing this ink onto an azide-functionalized surface [100].

More complex, multistep reactions can also be carried out with DPN, if one views the water meniscus itself as a reaction vessel. This is illustrated by the work of Ding *et al.* [101] who synthesized CdS nanostructures by dissolving sulfur and the cadmium precursors into the ink. The sulfur precursor, thioacetamide, formed H_2S in the meniscus during patterning and then reacted with the Cd^{2+} salt to form CdS, which was subsequently deposited onto the surface. This work was later extended to the growth of epitaxial CdS structures on mica [102], where the authors carefully controlled the patterning conditions in order to obtain single-crystal triangular nanoplates.

4.5 Noncovalent reactions by DPN

Aside from the reactions that result in a covalent bond between the ink molecule and substrate, DPN has been used to facilitate a number of non-covalent reactions. One example of this is metal-ion coordination by SAMs, where the authors patterned metal salts onto fluorescent SAMs in order to modulate their emissive properties [103]. So far, this has been the only instance of using DPN to form coordination bonds, though given the rich history of coordination chemistry, exploring this class of reactions by DPN could prove extremely fruitful.

The most common class of non-covalent reactions is physisorption. Physisorption occurs through weak van der Waals forces, and is a particularly appealing class of chemistry for lithography due to its substrate/molecule generality. It is important to note that all of the aqueous and non-aqueous liquid inks discussed in Section 3 (except ODT) interact with their respective surfaces via physisorption. The first demonstration was the printing of a fluorescent molecule (Rhodamine 6G, or R6G) onto glass [104]. This work elicited a flurry of follow-up papers by a variety of groups, including studies on the deposition of R6G onto mica [105] and SiO_x [32], fluoroscein onto gold [106], dodecylamine (DDA) onto mica [107], pyrrole onto silicon [108], explosives onto mica [31], peptides onto glass [109] and SiO_x [110], and various polymers onto SiO_x [58, 111, 112].

Of the inks patterned by physisorption, the case of depositing DDA onto mica is particularly interesting, as the features it formed were dendritic [107] instead of circular. The authors attributed this anomalous diffusion to rapid growth of DDA crystals on mica, which they posit could lead to fractal-shaped crystals once the spot size exceeded the domain size. Interestingly, they found that weak binding between the surface and ink molecule is a necessary but not sufficient condition for observing anomalous transport, as ODT deposition onto mica did not yield irregular features. This example serves not only to illustrate the novel studies that can be performed with DPN, but it also serves as a warning: while physisorption is quite substrate/ink general, it may still require careful experimental design if round, uniform features are desired.

While physisorptive inks will often form circular features, these features have three-dimensional extent, which is in contrast to the flat features formed by SAMs. While many small-molecule diffusive inks that do not normally form SAMs can be coerced into forming two-dimensional SAM-like features through careful control of deposition variables, there is no fundamental reason that these inks form flat features. As for larger molecular weight liquid inks, they are always observed to form domed features, where the height of the feature is controlled by the interfacial energy between the ink and the substrate.

One class of non-covalent inks that has been extensively studied are lipids, which have been deposited on a wide variety of substrates [113]. Lipid deposition, which must take place under high humidity (>70%) in order to allow the ink to flow from the tip, is an example of a system where covalent binding to a substrate should be avoided, as strong binding between the lipid bilayer and the substrate disrupts the lipid bilayer structure, which is necessary for mimicking cell surfaces [114].

5 Concluding remarks

In summary, we have outlined the current understanding of the physical transport phenomenon and chemical interactions that play a role in DPN. The specifics of these processes are as diverse as the materials that have been studied, but after fourteen years of study, coherent pictures are beginning to emerge. However, there are still many unanswered questions that warrant further study. Concerning the transport of diffusive vs. liquid inks, there is a great opportunity for both modeling and systematic experimental study to shed light on this distinction and fill in our understanding of viscous fluid flow from a tip to a surface. While we have drawn a division between diffusive and liquid inks, diffusion and fluid flow need not act independently and may both be important to consider for understanding the transport behavior of some materials. While a host of chemical reactions have been performed in the context of DPN, studies aimed at understanding the extent to which one can control the chemical environment at the tip of an AFM have not been undertaken. Understanding how to tailor the chemical interactions to a greater degree will

dramatically improve our ability to direct reactions for applications in both lithography and nanoscale combinatorial chemistry.

Acknowledgements C. A. M. acknowledges the U. S. Air Force Office of Scientific Research (AFOSR, Awards FA9550-12-1-0280 and FA9550-12-1-0141), the Defense Advanced Research Projects Agency (DARPA, Award N66001-08-1-2044) and the National Science Foundation (NSF, Awards DBI-1152139 and DMB-1124131) for support of this research. K. A. B. and X. L. gratefully acknowledges support from Northwestern University's International Institute for Nanotechnology. D. J. E. acknowledges the DoD and AFOSR for a National Defense Science and Engineering Graduate (NDSEG) Fellowship, 32 CFR 168a.

References

1. R. D. Piner, J. Zhu, F. Xu, S. H. Hong, and C. A. Mirkin, "Dip-pen" nanolithography, *Science*, 1999, 283(5402): 661
2. S. H. Hong, J. Zhu, and C. A. Mirkin, Multiple ink nanolithography: Toward a multiple-pen nano-plotter, *Science*, 1999, 286(5439): 523
3. D. S. Ginger, H. Zhang, and C. A. Mirkin, The evolution of dip-pen nanolithography, *Angew. Chem. Int. Ed.*, 2004, 43(1): 30
4. K. Salaita, Y. H. Wang, and C. A. Mirkin, Applications of dip-pen nanolithography, *Nature Nanotech.*, 2007, 2(3): 145
5. C. C. Wu, D. N. Reinhoudt, C. Otto, V. Subramaniam, and A. H. Velders, Strategies for patterning biomolecules with dip-pen nanolithography, *Small*, 2011, 7(8): 989
6. F. W. Huo, Z. J. Zheng, G. F. Zheng, L. R. Giam, H. Zhang, and C. A. Mirkin, Polymer pen lithography, *Science*, 2008, 321(5896): 1658
7. W. Shim, A. B. Braunschweig, X. Liao, J. N. Chai, J. K. Lim, G. F. Zheng, and C. A. Mirkin, Hard-tip, soft-spring lithography, *Nature*, 2011, 469(7331): 516
8. K. A. Brown, D. J. Eichelsdoerfer, W. Shim, B. Rasin, B. Radha, X. Liao, A. L. Schmucker, G. Liu, and C. A. Mirkin, A cantilever-free approach to dot-matrix nano printing, *Proc. Natl. Acad. Sci. USA*, 2013, 110(32): 12921
9. L. R. Giam and C. A. Mirkin, Cantilever-free scanning probe molecular printing, *Angew. Chem. Int. Ed.*, 2011, 50(33): 7482
10. J. Jang, G. C. Schatz, and M. A. Ratner, Liquid meniscus condensation in dip-pen nanolithography, *J. Chem. Phys.*, 2002, 116(9): 3875
11. S. K. Saha and M. L. Culpepper, An ink transport model for prediction of feature size in dip pen nanolithography, *J. Phys. Chem. C*, 2010, 114(36): 15364
12. B. L. Weeks, A. Noy, A. E. Miller, and J. J. De Yoreo, Effect of dissolution kinetics on feature size in dip-pen nanolithography, *Phys. Rev. Lett.*, 2002, 88(25): 255505
13. J. Y. Jang, S. H. Hong, G. C. Schatz, and M. A. Ratner, Self-assembly of ink molecules in dip-pen nanolithography: A diffusion model, *J. Chem. Phys.*, 2001, 115(6): 2721
14. N. Cho, S. Ryu, B. Kim, G. C. Schatz, and S. Hong, Phase of molecular ink in nanoscale direct deposition processes, *J. Chem. Phys.*, 2006, 124(2): 024714
15. H. Kim and J. Jang, Serial pushing model for the self-assembly in dip-pen nanolithography, *J. Phys. Chem. A*, 2009, 113(16): 4313
16. H. Kim, G. C. Schatz, and J. Jang, Simplistic model for the dendritic growth of a monolayer in dip pen nanolithography, *J. Phys. Chem. C*, 2010, 114(4): 1922
17. C. D. Wu, T. H. Fang, and J. F. Lin, Effect of chain length of self-assembled monolayers in dip-pen nanolithography using molecular dynamics simulations, *J. Colloid Interface Sci.*, 2011, 361(1): 316
18. J. R. Felts, S. Somnath, R. H. Ewoldt, and W. P. King, Nanometer-scale flow of molten polyethylene from a heated atomic force microscope tip, *Nanotechnology*, 2012, 23(21): 215301
19. G. Liu, Y. Zhou, R. S. Banga, R. Boya, K. A. Brown, A. J. Chipre, S. T. Nguyen, and C. A. Mirkin, The role of viscosity on polymer ink transport in dip-pen nanolithography, *Chem. Sci.*, 2013, 4(5): 2093
20. S. Rozhok, R. Piner, and C. A. Mirkin, Dip-pen nanolithography: What controls ink transport? *J. Phys. Chem. B*, 2003, 107(3): 751
21. E. J. Peterson, B. L. Weeks, J. J. De Yoreo, and P. V. Schwartz, Effect of environmental conditions on dip pen nanolithography of mercaptohexadecanoic acid, *J. Phys. Chem. B*, 2004, 108(39): 15206
22. B. L. Weeks, M. W. Vaughn, and J. J. DeYoreo, Direct imaging of meniscus formation in atomic force microscopy using environmental scanning electron microscopy, *Langmuir*, 2005, 21(18): 8096
23. B. L. Weeks and J. J. DeYoreo, Dynamic meniscus growth at a scanning probe tip in contact with a gold substrate, *J. Phys. Chem. B*, 2006, 110(21): 10231
24. S. Rozhok, P. Sun, R. Piner, M. Lieberman, and C. A. Mirkin, AFM study of water meniscus formation between an AFM tip and NaCl substrate, *J. Phys. Chem. B*, 2004, 108(23): 7814
25. O. A. Nafday, M. W. Vaughn, and B. L. Weeks, Evidence of meniscus interface transport in dip-pen nanolithography: An annular diffusion model, *J. Chem. Phys.*, 2006, 125(14): 144703
26. S. Chung, J. R. Felts, D. Wang, W. P. King, and J. J. De Yoreo, Temperature-dependence of ink transport during thermal dip-pen nanolithography, *Appl. Phys. Lett.*, 2011, 99(19): 193101
27. L. R. Giam, Y. Wang, and C. A. Mirkin, Nanoscale molecular transport: The case of dip-pen nanolithography, *J. Phys. Chem. A*, 2009, 113(16): 3779
28. J. R. Hampton, A. A. Dameron, and P. S. Weiss, Transport rates vary with deposition time in dip-pen nanolithography, *J. Phys. Chem. B*, 2005, 109(49): 23118

29. T. H. Wu, H. H. Lu, and C. W. Lin, Dependence of transport rate on area of lithography and pretreatment of tip in dip-pen nanolithography, *Langmuir*, 2012, 28(41): 14509
30. L. Huang, Y. H. Chang, J. J. Kakkassery, and C. A. Mirkin, Dip-pen nanolithography of high-melting-temperature molecules, *J. Phys. Chem. B*, 2006, 110(42): 20756
31. O. A. Nafday, R. Pitchimani, B. L. Weeks, and J. Haaheim, Patterning high explosives at the nanoscale, *Propellants Explos. Pyrotech.*, 2006, 31(5): 376
32. M. Su and V. P. Dravid, Colored ink dip-pen nanolithography, *Appl. Phys. Lett.*, 2002, 80(23): 4434
33. H. Jung, C. K. Dalal, S. Kuntz, R. Shah, and C. P. Collier, Surfactant activated dip-pen nanolithography, *Nano Lett.*, 2004, 4(11): 2171
34. R. McKendry, W. T. S. Huck, B. Weeks, M. Fiorini, C. Abell, and T. Rayment, Creating nanoscale patterns of dendrimers on silicon surfaces with dip-pen nanolithography, *Nano Lett.*, 2002, 2(7): 713
35. Z. Zheng, J. W. Jang, G. Zheng, and C. A. Mirkin, Topographically flat, chemically patterned PDMS stamps made by dip-pen nanolithography, *Angew. Chem. Int. Ed.*, 2008, 47(51): 9951
36. J. W. Jang, R. G. Sanedrin, A. J. Senesi, Z. Zheng, X. Chen, S. Hwang, L. Huang, and C. A. Mirkin, Generation of metal photomasks by dip-pen nanolithography, *Small*, 2009, 5(16): 1850
37. J. A. Chai, F. W. Huo, Z. J. Zheng, L. R. Giam, W. Shim, and C. A. Mirkin, Scanning probe block copolymer lithography, *Proc. Natl. Acad. Sci. USA*, 2010, 107(47): 20202
38. J. H. Lim and C. A. Mirkin, Electrostatically driven dip-pen nanolithography of conducting polymers, *Adv. Mater.*, 2002, 14(20): 1474
39. H. Nakashima, M. J. Higgins, C. O'Connell, K. Torimitsu, and G. G. Wallace, Liquid deposition patterning of conducting polymer ink onto hard and soft flexible substrates via dip-pen nanolithography, *Langmuir*, 2012, 28(1): 804
40. L. S. Jung and C. T. Campbell, Sticking probabilities in adsorption of alkanethiols from liquid ethanol solution onto gold, *J. Phys. Chem. B*, 2000, 104(47): 11168
41. A. J. Senesi, D. I. Rozkiewicz, D. N. Reinhoudt, and C. A. Mirkin, Agarose-assisted dip-pen nanolithography of oligonucleotides and proteins, *ACS Nano*, 2009, 3(8): 2394
42. L. Huang, A. B. Braunschweig, W. Shim, L. Qin, J. K. Lim, S. J. Hurst, F. Huo, C. Xue, J. W. Jang, and C. A. Mirkin, Matrix-assisted dip-pen nanolithography and polymer pen lithography, *Small*, 2010, 6(10): 1077
43. D. J. Eichelsdoerfer, K. A. Brown, R. Boya, W. Shim, and C. A. Mirkin, Tuning the spring constant of cantilever-free tip arrays, *Nano Lett.*, 2013, 13(2): 664
44. L. R. Giam, S. He, N. E. Horwitz, D. J. Eichelsdoerfer, J. Chai, Z. Zheng, D. Kim, W. Shim, and C. A. Mirkin, Positionally defined, binary semiconductor nanoparticles synthesized by scanning probe block copolymer lithography, *Nano Lett.*, 2012, 12(2): 1022
45. G. Liu, D. J. Eichelsdoerfer, B. Rasin, Y. Zhou, K. A. Brown, X. Liao, and C. A. Mirkin, Delineating the pathways for the site-directed synthesis of individual nanoparticles on surfaces, *Proc. Natl. Acad. Sci. USA*, 2013, 110(3): 887
46. A. Ivanisevic and C. A. Mirkin, "Dip-pen" nanolithography on semiconductor surfaces, *J. Am. Chem. Soc.*, 2001, 123(32): 7887
47. L. M. Demers, D. S. Ginger, S. J. Park, Z. Li, S. W. Chung, and C. A. Mirkin, Direct patterning of modified oligonucleotides on metals and insulators by dip-pen nanolithography, *Science*, 2002, 296(5574): 1836
48. H. T. Wang, O. A. Nafday, J. R. Haaheim, E. Tevaarwerk, N. A. Amro, R. G. Sanedrin, C. Y. Chang, F. Ren, and S. J. Pearton, Toward consductive traces: Dip Pen Nanolithography (R) of silver nanoparticle-based inks, *Appl. Phys. Lett.*, 2008, 93(14): 143105
49. A. Hernandez-Santana, E. Irvine, K. Faulds, and D. Graham, Rapid prototyping of poly(dimethoxysiloxane) dot arrays by dip-pen nanolithography, *Chem. Sci.*, 2011, 2(2): 211
50. The Merck Index – An Encyclopedia of Chemicals, Drugs, and Biologicals, Whitehouse Station: Merck and Co., Inc., 2001
51. Kirk-Othmer Encyclopedia of Chemical Technology, New York: John Wiley and Sons, 1994
52. D. R. Lide, Handbook of Chemistry and Physics, Cleveland, Ohio: Chemcial Rubber Publishing Co., 1948
53. F. Hamouda, H. Sahaf, S. Held, G. Barbillon, P. Gogol, E. Moyen, A. Aassime, J. Moreau, M. Canva, J. M. Lourtioz, M. Hanbücken, and B. Bartenlian, Large area nanopatterning by combined anodic aluminum oxide and soft UV-NIL technologies for applications in biology, *Microelectron. Eng.*, 2011, 88(8): 2444
54. A. K. Mehrotra, Correlation and prediction of the viscosity of pure hydrocarbons, *Can. J. Chem. Eng.*, 1994, 72(3): 554
55. C. J. Brinker, G. C. Frye, A. J. Hurd, and C. S. Ashley, Fundamentals of sol-gel dip coating, *Thin Solid Films*, 1991, 201(1): 97
56. P. V. Schwartz, Molecular transport from an atomic force microscope Tip: A comparative study of dip-pen nanolithography, *Langmuir*, 2002, 18(10): 4041
57. P. E. Sheehan and L. J. Whitman, Thiol diffusion and the role of humidity in "dip pen nanolithography", *Phys. Rev. Lett.*, 2002, 88(15): 156104
58. Q. Tang, S. Shi, H. Huang, and L. M. Zhou, Fabrication of highly oriented microstructures and nanostructures of ferroelectric P(VDF-TrFE) copolymer via dip-pen nanolithography, *Superlattices Microstruct.*, 2004, 36(1–3): 21
59. H. Jung, R. Kulkarni, and C. P. Collier, Dip-pen nanolithography of reactive alkoxysilanes on glass, *J. Am. Chem. Soc.*, 2003, 125(40): 12096

60. J. H. Lim, D. S. Ginger, K. B. Lee, J. Heo, J. M. Nam, and C. A. Mirkin, Direct-write dip-pen nanolithography of proteins on modified silicon oxide surfaces, *Angew. Chem. Int. Ed.*, 2003, 42(20): 2309
61. E. Bellido, R. de Miguel, J. Sesé, D. Ruiz-Molina, A. Lostao, and D. Maspoch, Nanoscale positioning of inorganic nanoparticles using biological ferritin arrays fabricated by dip-pen nanolithography, *Scanning*, 2010, 32(1): 35
62. J. Kim, Y. H. Shin, S. H. Yun, D. S. Choi, J. H. Nam, S. R. Kim, S. K. Moon, B. H. Chung, J. H. Lee, J. H. Kim, K. Y. Kim, K. M. Kim, and J. H. Lim, Direct-write patterning of bacterial cells by dip-pen nanolithography, *J. Am. Chem. Soc.*, 2012, 134(40): 16500
63. M. Yang, P. E. Sheehan, W. P. King, and L. J. Whitman, Direct writing of a conducting polymer with molecular-level control of physical dimensions and orientation, *J. Am. Chem. Soc.*, 2006, 128(21): 6774
64. W. K. Lee, L. J. Whitman, J. Lee, W. P. King, and P. E. Sheehan, The nanopatterning of a stimulus-responsive polymer by thermal dip-pen nanolithography, *Soft Matter*, 2008, 4(9): 1844
65. W. Shim, K. A. Brown, X. Zhou, B. Rasin, X. Liao, and C. A. Mirkin, Multifunctional cantilever-free scanning probe arrays coated with multilayer graphene, *Proc. Natl. Acad. Sci. USA*, 2012, 109(45): 18312
66. W. K. Lee, Z. Dai, W. P. King, and P. E. Sheehan, Maskless nanoscale writing of nanoparticletpolymer composites and nanoparticle assemblies using thermal nanoprobes, *Nano Lett.*, 2010, 10(1): 129
67. B. A. Nelson, W. P. King, A. R. Laracuente, P. E. Sheehan, and L. J. Whitman, Direct deposition of continuous metal nanostructures by thermal dip-pen nanolithography, *Appl. Phys. Lett.*, 2006, 88(3): 033104
68. P. E. Sheehan, L. J. Whitman, W. P. King, and B. A. Nelson, Nanoscale deposition of solid inks via thermal dip pen nanolithography, *Appl. Phys. Lett.*, 2004, 85(9): 1589
69. K. H. Kim, J. D. Kim, Y. J. Kim, S. H. Kang, S. Y. Jung, and H. Jung, Protein immobilization without purification via dip-pen nanolithography, *Small*, 2008, 4(8): 1089
70. K. Salaita, A. Amarnath, T. B. Higgins, and C. A. Mirkin, The effects of organic vapor on alkanethiol deposition via Dip-pen nanolithography, *Scanning*, 2010, 32(1): 9
71. X. Zhou, S. He, K. A. Brown, J. Mendez-Arroyo, F. Boey, and C. A. Mirkin, Locally altering the electronic properties of graphene by nanoscopically doping it with Rhodamine 6G, *Nano Lett.*, 2013, 13(4): 1616
72. J. R. Hampton, A. A. Dameron, and P. S. Weiss, Double-ink dip-pen nanolithography studies elucidate molecular transport, *J. Am. Chem. Soc.*, 2006, 128(5): 1648
73. A. Ulman, Formation and structure of self-assembled monolayers, *Chem. Rev.*, 1996, 96(4): 1533
74. L. H. Dubois and R. G. Nuzzo, Synthesis, structure, and properties of model organic surfaces, *Annu. Rev. Phys. Chem.*, 1992, 43(1): 437
75. J. C. Love, L. A. Estroff, J. K. Kriebel, R. G. Nuzzo, and G. M. Whitesides, Self-assembled monolayers of thiolates on metals as a form of nanotechnology, *Chem. Rev.*, 2005, 105(4): 1103
76. F. Schreiber, Structure and growth of self-assembling monolayers, *Prog. Surf. Sci.*, 2000, 65(5–8): 151
77. K. B. Lee, S. J. Park, C. A. Mirkin, J. C. Smith, and M. Mrksich, Protein nanoarrays generated by dip-pen nanolithography, *Science*, 2002, 295(5560): 1702
78. R. A. Vega, D. Maspoch, K. Salaita, and C. A. Mirkin, Nanoarrays of single virus particles, *Angew. Chem. Int. Ed.*, 2005, 44(37): 6013
79. L. R. Giam, M. D. Massich, L. Hao, L. Shin Wong, C. C. Mader, and C. A. Mirkin, Scanning probe-enabled nanocombinatorics define the relationship between fibronectin feature size and stem cell fate, *Proc. Natl. Acad. Sci. USA*, 2012, 109(12): 4377
80. C. L. Cheung, J. A. Camarero, B. W. Woods, T. Lin, J. E. Johnson, and J. J. De Yoreo, Fabrication of assembled virus nanostructures on templates of chemoselective linkers formed by scanning probe nanolithography, *J. Am. Chem. Soc.*, 2003, 125(23): 6848
81. L. S. Wong, C. V. Karthikeyan, D. J. Eichelsdoerfer, J. Micklefield, and C. A. Mirkin, A methodology for preparing nanostructured biomolecular interfaces with high enzymatic activity, *Nanoscale*, 2012, 4(2): 659
82. D. J. Pena, M. P. Raphael, and J. M. Byers, "Dip-pen" nanolithography in registry with photolithography for biosensor development, *Langmuir*, 2003, 19(21): 9028
83. K. Salaita, A. Amarnath, D. Maspoch, T. B. Higgins, and C. A. Mirkin, Spontaneous "phase separation" of patterned binary alkanethiol mixtures, *J. Am. Chem. Soc.*, 2005, 127(32): 11283
84. S. W. Lee, B. K. Oh, R. G. Sanedrin, K. Salaita, T. Fujigaya, and C. A. Mirkin, Biologically active protein nanoarrays generated using parallel dip-pen nanolithography, *Adv. Mater.*, 2006, 18(9): 1133
85. J. W. Jang, D. Maspoch, T. Fujigaya, and C. A. Mirkin, A "molecular eraser" for dip-pen nanolithography, *Small*, 2007, 3(4): 600
86. J.-W. Jang, J. M. Collins, and S. Nettikadan, User-friendly universal and durable subcellular-scaled template for protein binding: Application to single-cell patterning, *Adv. Funct. Mater.*, 2013, DOI: 10.1002/adfm.201301088
87. S. E. Kooi, L. A. Baker, P. E. Sheehan, and L. J. Whitman, Dip-pen nanolithography of chemical templates on silicon oxide, *Adv. Mater.*, 2004, 16(12): 1013
88. Y. Cho and A. Ivanisevic, Peptides on GaAs surfaces: Comparison between features generated by microcontact printing and dip-pen nanolithography, *Langmuir*, 2006, 22(21): 8670
89. H. P. Wampler, D. Y. Zemlyanov, and A. Ivanisevic, Comparison between patterns generated by microcontact printing and dip-pen nanolithography on InP surfaces, *J. Phys. Chem. C*, 2007, 111(49): 17989

90. R. Flores-Perez, D. Y. Zemlyanov, and A. Ivanisevic, Lithography on GaP(100) surfaces, *Surf. Sci.*, 2008, 602(11): 1993

91. J. W. J. Slavin and A. Ivanisevic, Dip-pen nanolithography on etched InAs(100) using homogeneous and mixed ink solutions, *J. Vac. Sci. Technol. B*, 2009, 27(3): 1215

92. S. Matsubara, H. Yamamoto, K. Oshima, E. Mouri, and H. Matsuoka, Fabrication of nano-structure by diels–alder reaction, *Chem. Lett.*, 2002, 31(9): 886

93. G. H. Degenhart, B. Dordi, H. Schönherr, and G. J. Vancso, Micro- and nanofabrication of robust reactive arrays based on the covalent coupling of dendrimers to activated monolayers, *Langmuir*, 2004, 20(15): 6216

94. Y. S. Chi and I. S. Choi, Dip-pen nanolithography using the amide-coupling reaction with interchain carboxylic anhydride-terminated self-assembled monolayers, *Adv. Funct. Mater.*, 2006, 16(8): 1031

95. L. K. Blasdel, S. Banerjee, and S. S. Wong, Selective borohydride reduction using functionalized atomic force microscopy tips, *Langmuir*, 2002, 18(13): 5055

96. A. B. Braunschweig, A. J. Senesi, and C. A. Mirkin, Redox-activating dip-pen nanolithography (RA-DPN), *J. Am. Chem. Soc.*, 2009, 131(3): 922

97. B. W. Maynor, Y. Li, and J. Liu, Au "ink" for AFM "dip-pen" nanolithography, *Langmuir*, 2001, 17(9): 2575

98. H. C. Kolb, M. G. Finn, and K. B. Sharpless, Click chemistry: Diverse chemical function from a few good reactions, *Angew. Chem. Int. Ed.*, 2001, 40(11): 2004

99. D. A. Long, K. Unal, R. C. Pratt, M. Malkoch, and J. Frommer, Localized "click" chemistry through dip-pen nanolithography, *Adv. Mater.*, 2007, 19(24): 4471

100. S. Bian, J. He, K. B. Schesing, and A. B. Braunschweig, Polymer pen lithography (ppl)-induced site-specific click chemistry for the formation of functional glycan arrays, *Small*, 2012, 8(13): 2000

101. L. Ding, Y. Li, H. Chu, X. Li, and J. Liu, Creation of cadmium sulfide nanostructures using afm dip-pen nanolithography, *J. Phys. Chem. B*, 2005, 109(47): 22337

102. H. Chu, L. Ding, J. Wang, X. Li, L. You, and Y. Li, In situ epitaxial growth of triangular CdS nanoplates on mica by dip-pen nanolithography, *J. Phys. Chem. C*, 2008, 112(48): 18938

103. L. Basabe-Desmonts, C. C. Wu, K. O. van der Werf, M. Peter, M. Bennink, C. Otto, A. H. Velders, D. N. Reinhoudt, V. Subramaniam, and M. Crego-Calama, Fabrication and visualization of metal-ion patterns on glass by dip-pen nanolithography, *ChemPhysChem*, 2008, 9(12): 1680

104. A. Noy, A. E. Miller, J. E. Klare, B. L. Weeks, B. W. Woods, and J. J. DeYoreo, Fabrication of luminescent nanostructures and polymer nanowires using dip-pen nanolithography, *Nano Lett.*, 2002, 2(2): 109

105. H. Zhou, Z. Li, A. Wu, G. Wei, and Z. Liu, Direct patterning of rhodamine 6G molecules on mica by dip-pen nanolithography, *Appl. Surf. Sci.*, 2004, 236(1–4): 18

106. A. Martínez-Otero, J. Hernando, D. Ruiz-Molina, and D. Maspoch, pH-responsive fluorescent nanoarrays fabricated by direct-write parallel dip-pen nanolithography, *Small*, 2008, 4(12): 2131

107. P. Manandhar, J. Jang, G. C. Schatz, M. A. Ratner, and S. Hong, Anomalous surface diffusion in nanoscale direct deposition processes, *Phys. Rev. Lett.*, 2003, 90(11): 115505

108. M. Su, M. Aslam, L. Fu, N. Q. Wu, and V. P. Dravid, Dip-pen nanopatterning of photosensitive conducting polymer using a monomer ink, *Appl. Phys. Lett.*, 2004, 84(21): 4200

109. G. Agarwal, L. A. Sowards, R. R. Naik, and M. O. Stone, Dip-pen nanolithography in tapping mode, *J. Am. Chem. Soc.*, 2003, 125(2): 580

110. H. Jiang and S. I. Stupp, Dip-pen patterning and surface assembly of peptide amphiphiles, *Langmuir*, 2005, 21(12): 5242

111. M. Yu, D. Nyamjav, and A. Ivanisevic, Fabrication of positively and negatively charged polyelectrolyte structures by dip-pen nanolithography, *J. Mater. Chem.*, 2005, 15(6): 649

112. S. W. Lee, R. G. Sanedrin, B. K. Oh, and C. A. Mirkin, Nanostructured polyelectrolyte multilayer organic thin films generated via parallel dip-pen nanolithography, *Adv. Mater.*, 2005, 17(22): 2749

113. S. Lenhert, P. Sun, Y. H. Wang, H. Fuchs, and C. A. Mirkin, Massively parallel dip-pen nanolithography of heterogeneous supported phospholipid multilayer patterns, *Small*, 2007, 3(1): 71

114. M. Tanaka and E. Sackmann, Polymer-supported membranes as models of the cell surface, *Nature*, 2005, 437(7059): 656